ISSN 1067-8212, Russian Journal of Non-Ferrous Metals, 2021, Vol. 62, No. 5, pp. 531–538. © Allerton Press, Inc., 2021.
Russian Text © The Author(s), 2021, published in Izvestiya Vysshikh Uchebnykh Zavedenii, Tsvetnaya Metallurgiya, 2021, No. 4, pp. 42–50.

PHYSICAL METALLURGY AND HEAT TREATMENT

Effect of Annealing Temperature and Time on Martensitic Transformation Temperatures and Mechanical Properties of the Ti–50.7 at % Ni Shape Memory Alloy

K. A. Polyakova[a], * and V. S. Komarov[a], **

[a] *National University of Science and Technology MISIS, Moscow, 119991 Russia*

**e-mail: vachiyan@yandex.ru*

***e-mail: komarov@misis.ru*

Received May 13, 2021; revised May 16, 2021; accepted May 17, 2021

Abstract—The influence of temperature and time of recrystallization annealing on the characteristic temperatures of martensitic transformation and mechanical properties has been studied using Ti–50.7 at % Ni shape memory alloy in the form of wire after cold deformation by drawing at room temperature. Six regimes of post-deformation annealing have been considered for the alloy at various temperatures and holding times; as a consequence, structures with various sizes of recrystallization grain have been obtained. Its size is determined by electron backscatter diffraction (EBSD); it has been revealed that it increases from 2.5 μm to 9 μm upon an increase in both the annealing temperature (600–700°C) and the holding time (0.5–5.0 h). The characteristic temperatures of forward and reverse martensitic transformations have been determined by differential scanning calorimetry. It has been demonstrated that, as a consequence of a threefold increase in the size of recrystallized grain, the martensite start temperature decreases and the temperature range of reverse martensitic transformation is broadened. The results of mechanical tension tests at ambient temperature evidence that the increase in grain size results in a decrease in the dislocation yield strength and an increase in the yield strength. It has been determined that the dislocation yield strength is defined by the Hall–Petch law and the phase yield strength by the position of testing temperature with regard to the temperature of the start (or peak) of forward martensitic transformation. While recommending the heat treatment regime for certain products, these competing factors should be taken into account along with the temperatures of reverse martensitic transformation responsible for the temperatures of shape recovery.

Keywords: Ti–Ni shape memory alloys, titanium nickelide, cold deformation, post-deformation annealing, mechanical properties, martensitic transformations

DOI: 10.3103/S1067821221050114

INTRODUCTION

Titanium-based shape memory alloys (SMA) are promising materials for medical equipment [1–4]. The most common among them is hyper-equatomic Ti–Ni alloy (titanium nickelide) applied in medical apparatuses [5–9]. The response temperature of these elements should correspond to that of the human body, and this is provided by Ti–50.7 at % Ni alloy—hyper eutectic in terms of nickel.

It is known that the grain size of the initial phase (*B*2 austenite) influences the functional and mechanical properties of Ti–Ni SMA [10–18]. It was demonstrated in [12] that, in Ti–50.8 at % Ni alloy after cold drawing with 25% reduction and annealing at t = 700°C with holding time from 3 min to 24 h, the start temperature of martensitic transformation remains nearly unchanged as a consequence of the increase in grain size from 5 to 22 μm, and additional ageing at t = 250°C, τ = 24 h changes the staging of martensitic transformations. At the same time, the authors [13, 14] revealed that the initial size of recrystallized grain in the range of 5–15 μm influences the distribution of particles of the Ti_3Ni_4 phase, the kinetics of martensitic transformations, as well as the functional properties of Ti–50.7 at % Ni SMA.

The insufficient amount of required information determines the aim of the present study: to understand how various temperatures and times of annealing, hence, the size of recrystallized grain of *B*2 austenite, can influence the properties of martensitic transformations and mechanical behavior of Ti–Ni SMA.

EXPERIMENTAL

Titanium nickelide Ti–50.7 at % Ni was analyzed in the form of wire with the diameter of 0.3 mm after cold deformation at room temperature with true (logarithmic) accumulated strain e = 0.6. Post-deforma-

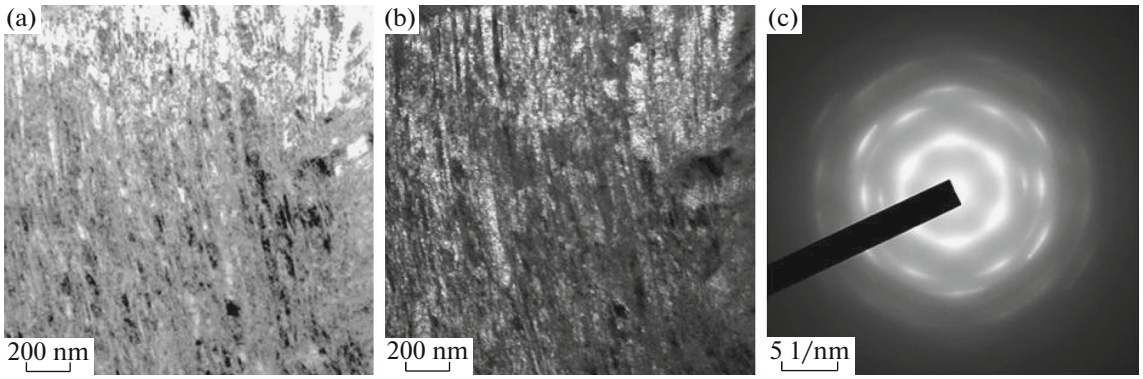

Fig. 1. Initial microstructure of Ti–50.7 at % Ni alloy after cold drawing with true (logarithmic) accumulated strain $e = 0.6$: (a) bright field image, (b) dark field image, and (c) diffraction pattern.

tion annealing was carried out at 600 and 700°C and a holding time in the range of $\tau = 0.5–5.0$ h in order to obtain a recrystallized grain of different size. Cooling in water was carried out after annealing.

The grain size was determined by electron backscatter diffraction (EBSD) using a TSL-EDAX system on a TESCAN scanning electron microscope (Czech Republic). The samples were mechanically polished using paper of various grain sizes (from P320 to P2500) and subsequent electrolytic polishing in an electrolyte solution comprised of 30% nitric acid and 70% methanol. The electric polishing was carried out at $t = -20$°C and voltage of 20 V in 30 s. The grain size (d) was determined by the secant method with sampling of at least 300 grains.

The characteristic temperatures of martensitic transformations are as follows:

M_s, M_p, and M_f—start, peak, and finish of forward martensitic transformation,

A_s, A_p, and A_f—start, peak, and finish of reverse martensitic transformation,

estimated by a Mettler Toledo 822e differential scanning calorimeter (Switzerland). The heating/cooling rate was 10°C/min.

The failure strain tests were carried out with wire samples with a diameter of 0.3 mm and length of 100 mm (working part 50 mm) using an Instron 5966 universal testing machine (Great Britain) at a rate of 2 mm/min at ambient temperature.

Table 1. Regimes of recrystallization annealing

t_{anneal}, °C	τ, h			
600	–	–	2.0	5.0
700	0.5	1.0	2.0	5.0

RESULTS AND DISCUSSION

In the course of cold drawing with strain $e = 0.6$ (cross-section reduction of 45%), the developed dislocation substructure of $B2$ austenite is formed (Fig. 1). Halo can be observed in the diffraction pattern evidencing partial amorphization of the structure.

Aiming at the formation of recrystallized grain of different sizes, two annealing temperatures were selected ($t_{anneal} = 600$ and 700°C) with various holding times ($\tau = 0.5–5.0$) (Table 1).

As a consequence of post-deformation annealing at 600 and 700°C, the fine-grain recrystallized structure of B2 austenite is observed (Fig. 2). The grain sizes are summarized in Fig. 3. It follows from the presented data that, as a consequence of annealing at 600°C in 2 and 5 h, a minor increase in the grain size from 2.7 to 3.0 μm is observed. In the regime of $t_{anneal} = 600$°C, $\tau = 2$ h, a small amount of fine grains was formed from 500 nm to 1 μm in size (see Fig. 2). When the holding time was increased to 5 h, their amount slightly decreased; however, the changes in the grain structure are insignificant.

With an increase in the annealing temperature to 700°C, by a 30-min holding time the average grain size is doubled (up to 5.6 μm); with a further increase in the holding time to 1 and 2 h, the grain sizes gradually increased to 6.2 and 6.5 μm; grains finer than 1 μm (Fig. 2) are nearly absent. In the regime of $t_{anneal} =$ 700°C, $\tau = 5$ h, the grain size reaches ~8.6 μm.

Figure 4 illustrates calorimetric cooling curves of titanium nickelide alloy as a consequence of post-deformation annealing as a function of the size of recrystallized grain (d), and Table 2 shows characteristic temperatures of martensitic transformations of the alloy. In all cases (except for annealing at 600°C, $\tau = 2$ h), one stage $B2 \rightarrow B19'$ transformation is observed upon cooling and, upon heating, $B19' \rightarrow B2$ transformation (Figs. 4–6). The transformation after annealing at $t_{anneal} = 600$°C, $\tau = 2$ h starts from the formation of a minor amount of intermediate R phase,

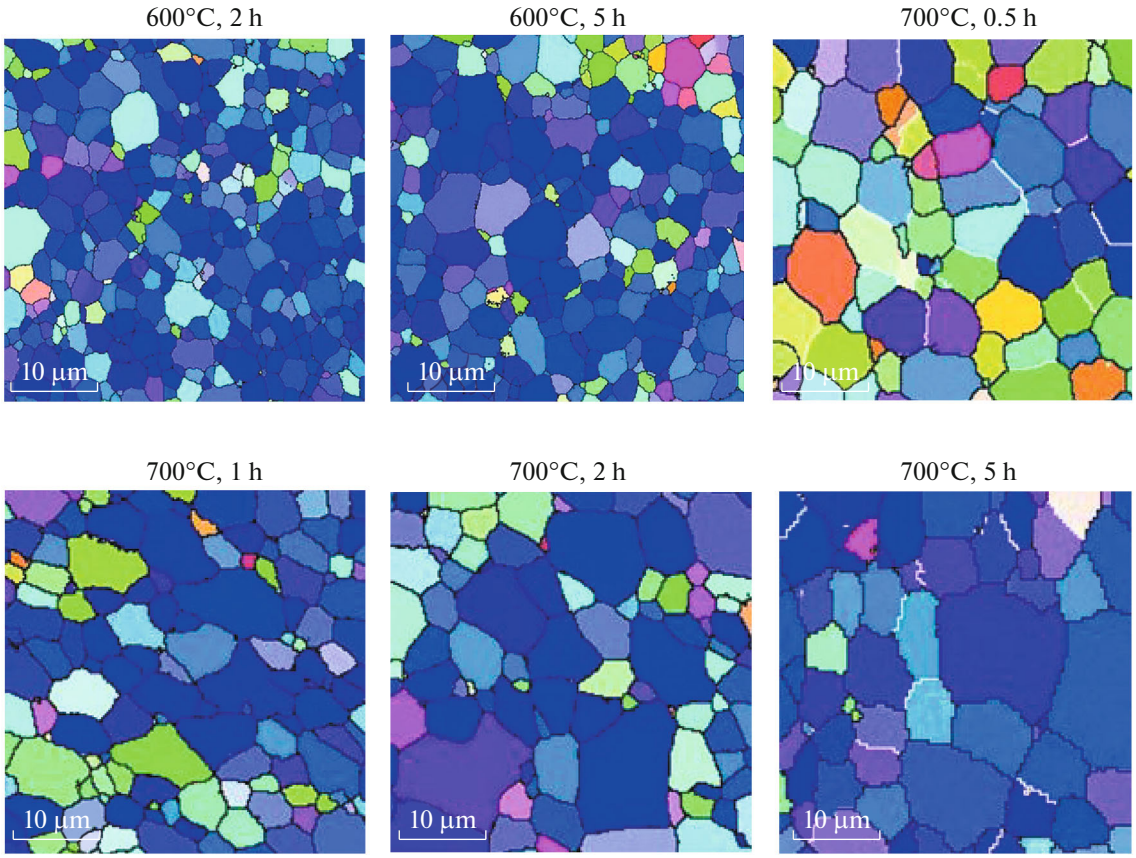

Fig. 2. Alloy structure after cold drawing deformation and annealing at various temperatures and times.

which is rapidly (in 5°) replaced with the formation of *B*19' martensite.

Figure 5 illustrated the temperatures of forward and reverse martensitic transformations as a function of the annealing temperature and holding time.

As a consequence of the increase in the annealing time from 2 to 5 h at t_{anneal} = 600°C, the start temperature of forward martensitic transformation (M_s) increases from 9 to 16°C and the peal temperature of *B*2 → *B*19' transformation increases from 5 to 11°C. The start and finish temperatures of reverse martensitic transformation also increase from 20 to 26°C (A_s) and from 36 to 42°C (A_f).

With an increase in the holding time from 0.5 to 5 h at t_{anneal} = 700°C, temperature M_s decreases from –21 to –31°C. Herewith, the peak temperature of B2→B19' transformation decreases from –29 to –34°C at τ = 5 h. The start temperature of reverse martensitic transformation (A_s) decreases to the region of low values from –23 to –56°C with an increase in τ from 1 to 5 h, and the finish temperature (A_f) remains the same at an annealing time of 1–2 h, but decreases to –7°C at a holding time of 5 h.

Therefore, it is possible to conclude that the size of recrystallized grain in the range of *d* = 2.5–9 μm influ-

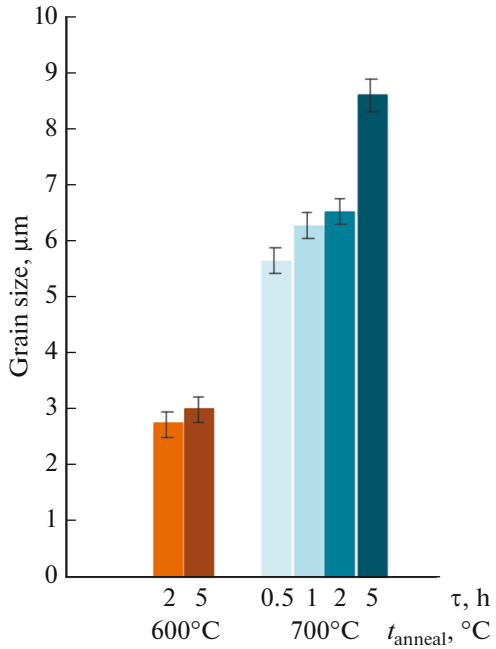

Fig. 3. Grain size as a function of temperature and time of annealing.

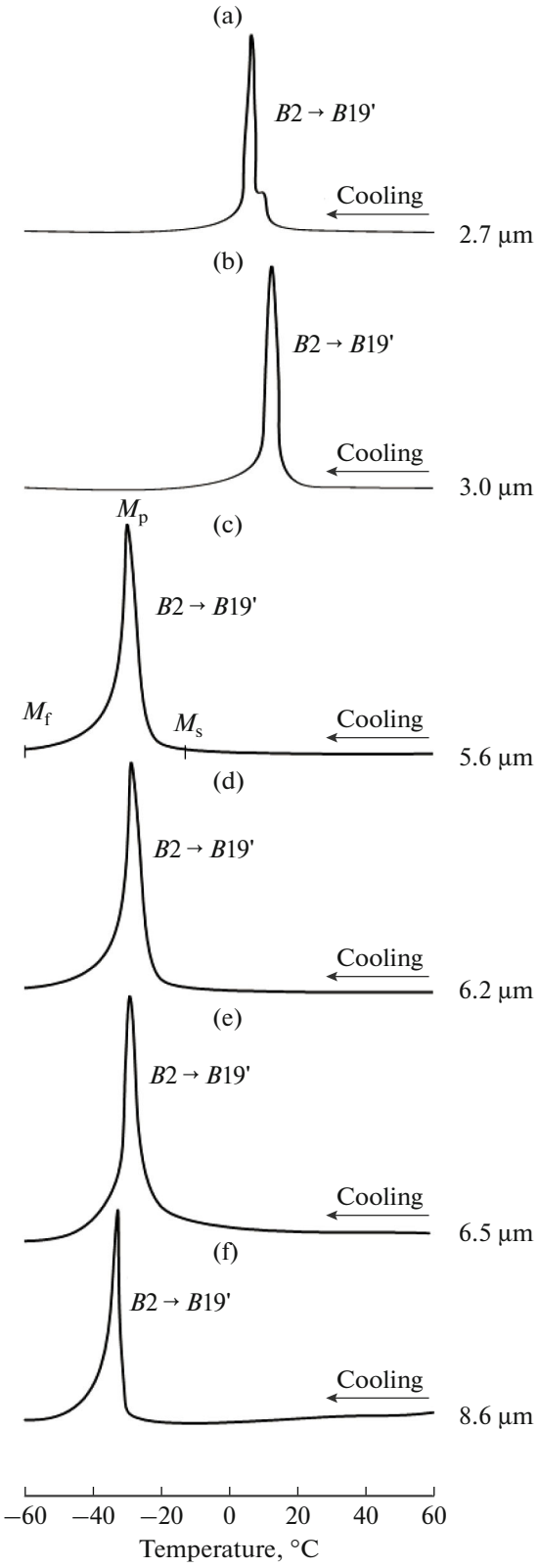

Fig. 4. Cooling curves of Ti–50.7 at % Ni alloy after annealing according to the considered regimes: (a) t_{anneal} = 600°C, τ = 2 h; (b) 600°C and 5 h; (c) 700°C and 0.5 h; (d) 700°C and 1 h; (e) 700°C and 2 h; (f) 700°C and 5 h.

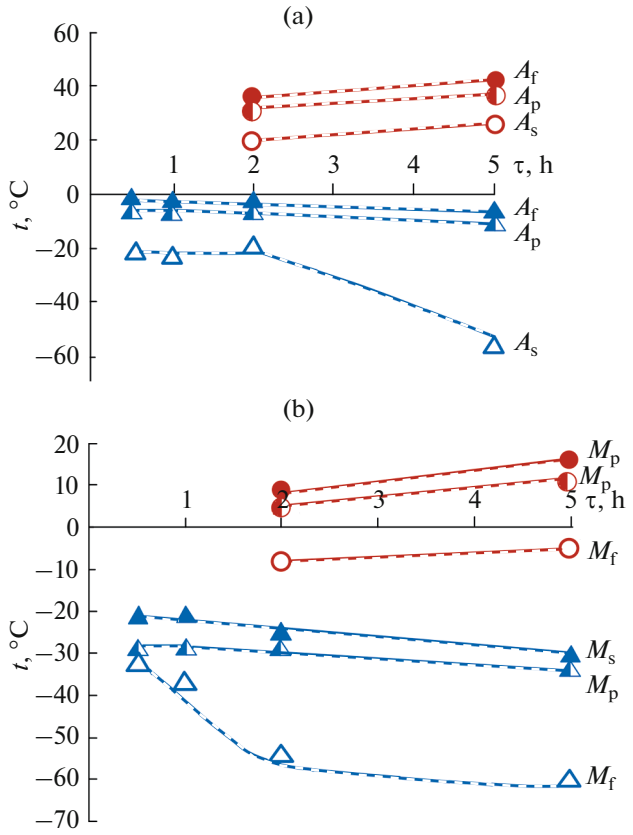

Fig. 5. Temperatures of forward (a) and reverse (b) martensitic transformations as a function of annealing temperature and holding time: t_{anneal} = 600°C (solid lines); t_{anneal} = 700°C (dashed lines).

ences the temperatures of martensitic transformations. As a consequence of the twofold size increase of the recrystallized grain from 2.7 μm (t_{anneal} = 600°C, τ = 2 h) to 5.5 μm (700°C, 1 h), the start temperature of forward martensitic transformation decreases from 9 to –21°C.

Figure 6 illustrates the stress strain curves after annealing at various temperatures and holding times.

The influence of post-deformation annealing on the mechanical behavior of Ti–50.7 at % Ni alloy is summarized in Table 3. It follows that, with an increase in t_{anneal} from 600 to 700°C, τ = 0.5 h, the phase yield strength increases and the dislocation yield strength decreases. If the decrease in σ_d seems natural, since it correlates with a sharp increase in grain size, then the increase of σ_{ph} under the same conditions seemingly contradicts grain coarsening. In order to explain the differences in the mentioned regularities, it should be mentioned that, in addition to the grain size, the important factor influencing the phase yield strength of SMA is the difference between the testing temperature and the start (or peak) temperature of forward martensitic transformation $\Delta t = t_{test} - M_p$ in

Table 2. Characteristic temperatures of martensitic transformations in Ti–50.7 at % Ni alloy

Heat-treatment regime t_{anneal}, τ	d, μm	Temperature, °C					
		cooling ($B2 \rightarrow B19'$)			heating ($B19' \rightarrow B2$)		
		M_p	M_s	M_f	A_p	A_s	A_f
600°C, 2 h	2.7	5	9	–8	32	20	36
600°C, 5 h	3.0	11	16	–5	37	26	42
700°C, 0.5 h	5.6	–29	–21	–34	–4	–15	–1
700°C, 1 h	6.2	–29	–21	–37	–7	–23	–3
700°C, 2 h	6.5	–29	–26	–54	–7	–19	–3
700°C, 5 h	8.6	–34	–31	–60	–11	–56	–7

accordance with the Clapeyron–Clausius equation: the higher it is, the higher the phase yield strength is [19].

As can be seen in Fig. 7, σ_{ph} linearly increases with an increase in Δt directly corresponding to the Clapeyron–Clausius equation. Hence, the main factor determining the phase yield strength is the difference between the testing temperature and the temperature of martensitic transformation; the grain size is a secondary factor.

It can be seen in Fig. 8 that the dislocation yield strength as a function of grain size corresponds the Hall–Petch law ($\sigma_s \sim 1/\sqrt{d}$) and is linearized in the σ–$1/\sqrt{d}$ coordinates [20–23].

Therefore, the results make it possible to conclude that, upon selecting a regime of heat treatment to achieve the required level of mechanical and functional properties of Ti–50.7 at % Ni SMA, two competing factors influencing the dislocation and the phase yield strengths should be considered: the first (σ_d) is determined mainly by grain size and obeys the Hall–Petch law and the second (σ_{ph}) is determined mainly by the position of the deformation temperature inducing the shape memory effect with regard to the start temperature of forward martensitic transformation. The phase yield strength decreases while

Table 3. Mechanical properties* of Ti–50.7 at % Ni alloy

Heat-treatment regime t_{anneal}, τ	σ_{ph}, MPa	σ_d, MPa	$\Delta\sigma$	σ_u, MPa	δ, %
600°C, 2 h	105	560	455	1000	57
600°C, 5 h	90	560	470	1000	61
700°C, 0.5 h	380	430	50	1100	65
700°C, 1 h	290	350	60	1000	64
700°C, 2 h	290	350	60	950	60
700°C, 5 h	320	350	30	900	52

*Notes: σ_{ph}, phase yield strength; σ_d, dislocation yield strength; $\Delta\sigma = \sigma_d, \sigma_{ph}$, difference between dislocation and phase yield strengths characterizing the extent of possible achievement of the resource of reverse deformation; σ_u, ultimate strength; and δ, relative elongation.

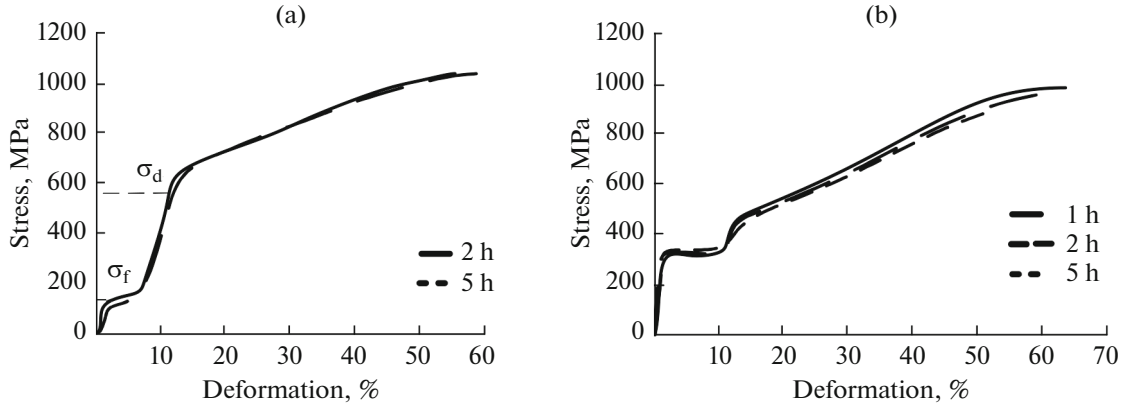

Fig. 6. Stress–strain curves of Ti–50.7 at % Ni alloy before destruction at ambient temperature as a function of annealing temperatures of 600 (a), 700°C (b), and holding time.

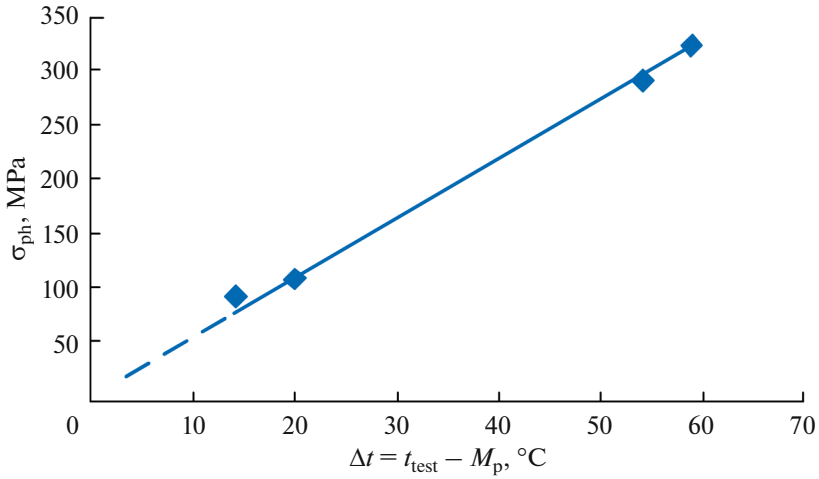

Fig. 7. Phase yield strength of Ti–50.7 at % Ni alloy as a function of the difference between testing temperature and peak temperature of forward martensitic transformation.

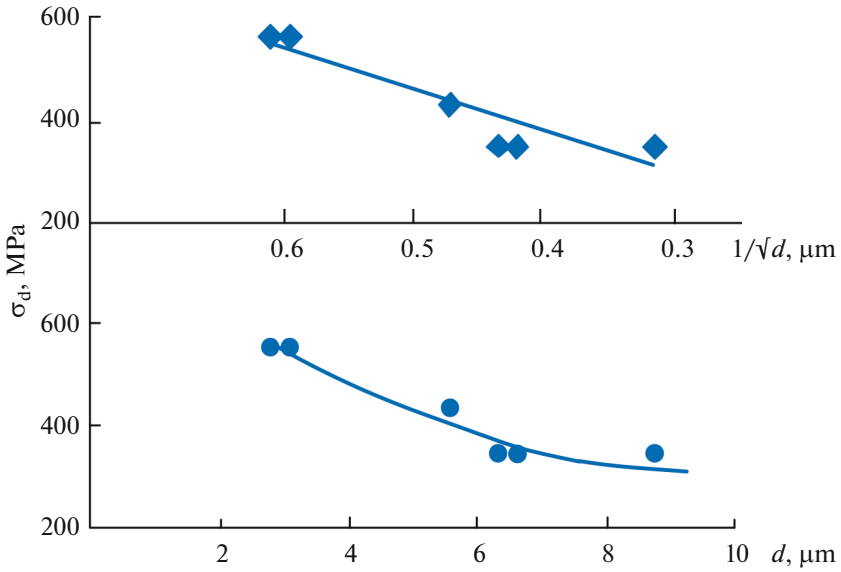

Fig. 8. Dislocation yield strength as a function of grain size.

approaching temperature M_s from both high and low temperatures.

CONCLUSIONS

(1) The recrystallized structure of $B2$ austenite is formed in Ti–50.7 at % Ni shape memory alloy as a consequence of cold drawing deformation with true (logarithmic) accumulated strain $e = 0.6$ and post-deformation annealing at 600–700°C in 0.5–5.0 h; the size of recrystallized grains (d) increases from 2.5 to 9 μm.

(2) The size of recrystallized grain in the range from 2.5 to 9 μm influences the characteristic temperatures of martensitic transformations. As a consequence of the threefold increase of d from 2.7 (t_{anneal} = 600°C, τ = 2 h) to 8.6 μm (700°C, 5 h), the start temperature of forward martensitic transformation decreases from 9 to –31°C. Herewith, the dislocation yield strength decreases and the phase yield strength increases.

(3) Upon selecting a regime of heat treatment to achieve the required level of mechanical and functional properties of Ti–50.7 at % Ni SMA, it is required to take into account that the dislocation yield strength is determined mainly by grain size and obeys the Hall–Petch law and the phase yield strength (in accordance with the Clapeyron–Clausius equation) is determined mainly by the position of the temperature of deformation inducing the shape memory

effect with regard to the start temperature of forward martensitic transformation.

ACKNOWLEDGMENTS

We are grateful to N. Resnina (St. Petersburg State University) for her assistance in performing calorimetric studies.

FUNDING

This work was supported by the Russian Science Foundation (project no. 19-79-00365).

CONFLICT OF INTEREST

The authors declare that the presented data do not contain any conflict of interest.

REFERENCES

1. Miyazaki, S., My experience with Ti-Ni-based and Ti-based shape memory alloys, *Shape Mem. Superelasticity,* 2017, vol. 3, pp. 279–314. https://doi.org/10.1007/s40830-017-0122-3
2. Gunderov, D., Prokoshkin, S., Churakova, A., Sheremetyev, V., and Ramazanov, I., Effect of HPT and accumulative HPT on structure formation and microhardness of the novel Ti18Zr15Nb alloy, *Mater. Lett.,* 2021, vol. 283, article no. 128819. https://doi.org/10.1016/j.matlet.2020.128819
3. Sheremetyev, V., Petrzhik, M., Zhukova, Y., Kazakbiev, A., Arkhipova, A., Moisenovich, M., Prokoshkin, S., and Brailovski, V., Structural, physical, chemical, and biological surface characterization of thermomechanically treated Ti–Nb-based alloys for bone implants, *J. Biomed. Mater. Res., Part B,* 2020, vol. 108, no. 3, pp. 647–662. https://doi.org/10.1002/jbm.b.34419
4. Kudryashova, A., Sheremetyev, V., Lukashevich, K., Cheverikin, V., Inaekyan, K., Galkin, S., Prokoshkin, S., and Brailovski, V., Effect of a combined thermomechanical treatment on the microstructure, texture and superelastic properties of Ti–18Zr–14Nb alloy for orthopedic implants, *J. Alloys Compd.,* 2020, vol. 843, article no. 156066. https://doi.org/10.1016/j.jallcom.2020.156066
5. Ryklina, E., Korotitskiy, A., Khmelevskaya, I., Prokoshkin, S., Polyakova, K., Kolobova, A., Soutorine, M., and Chernov, A., Control of phase transformations and microstructure for optimum realization of one-way and two-way shape memory effects in removable surgical clips, *Mater. Des.,* 2017, vol. 136, pp. 174–184. https://doi.org/10.1016/j.matdes.2017.09.024
6. Ryklina, E.P., Khmelevskaya, I.Yu., Prokoshkin, S.D., Inaekyan, K.E., and Ipatkin, R.V., Effects of strain aging on two-way shape memory effect in a nickel-titanium alloy for medical application, *Mater. Sci. Eng., A,* 2006, vols. 438–440, pp. 1093–1096.
7. Khmelevskaya, I.Yu., Ryklina, E.P., Prokoshkin, S.D., Markossian, G.A., Tarutta, E.P., and Iomdina, E.N., A shape memory device for the treatment of high myopia, *Mater. Sci. Eng., A,* 2008, vols. 481–482, nos. 1–2, pp. 651–653.
8. Komarov, V., Khmelevskaya, I., Karelin, R., Kawalla, R., Korpala, G., Prahl, U., Yusupov, V., and Prokoshkin, S., Deformation behavior, structure, and properties of an aging Ti–Ni shape memory alloy after compression deformation in a wide temperature range, *JOM,* 2021, vol. 73, no. 2, pp. 620–629. https://doi.org/10.1007/s11837-020-04508-7
9. Karelin, R.D., Khmelevskaya, I.Y., Komarov, V.S., Andreev, V.A., Perkas, M.M., Yusupov, V.S., and Prokoshkin, S.D., Effect of quasi-continuous equal-channel angular pressing on structure and properties of Ti-Ni shape memory alloys, *J. Mater. Eng. Perform.,* 2021, vol. 30, no. 4, pp. 3096–3106. https://doi.org/10.1007/s11665-021-05625-3
10. Belyaev, S., Resnina, N., Saveleva, A., Glazova, D., and Pilyugin, V., Influence of the grain size on the strain variation on cooling and heating of Ni50.2Ti49.8 alloy under stress, *Mater. Sci. Eng., A,* 2019, vol. 759, pp. 778–784. https://doi.org/10.1016/j.msea.2019.05.061
11. Belyaev, S., Resnina, N., Pilyugin, V., Glazova, D., Zeldovich, V., and Frolova, N., Shape memory effects in Ti–50.2 at% Ni alloy with different grain size, *Mater. Sci. Eng., A,* 2017, vol. 706, pp. 64–70. https://doi.org/10.1016/j.msea.2017.08.113
12. Wang, X., Li, C., Verlinden, B., and Van Humbeeck, J., Effect of grain size on aging microstructure as reflected in the transformation behavior of a low-temperature aged Ti–50.8 at % Ni alloy, *Scr. Mater.,* 2013, vol. 69, no. 7, pp. 545–548. https://doi.org/10.1016/j.scriptamat.2013.06.023
13. Polyakova, K.A., Ryklina, E.P., and Prokoshkin, S.D., Effect of grain size and ageing-induced microstructure on functional characteristics of a Ti–50.7 at % Ni alloy, *Shape Mem. Superelasticity,* 2020, vol. 6, no. 1, pp. 139–147. https://doi.org/10.1007/s40830-020-00269-z
14. Ryklina, E.P., Polyakova, K.A., Tabachkova, N.Yu., Resnina, N.N., and Prokoshkin, S.D., Effect of B2 austenite grain size and aging time on microstructure and transformation behavior of thermomechanically treated titanium nickelide, *J. Alloys Compd.,* 2018, vol. 764, pp. 626–638. https://doi.org/10.1016/j.jallcom.2018.06.102
15. Resnina, N., Belyaev, S., Pilugin, V., and Glazova, D., Mechanical behavior of nanostructured TiNi shape memory alloy with different grain size, *Mater. Today: Proc.,* 2017, vol. 4, no. 3, pp. 4841–4845. https://doi.org/10.1016/j.matpr.2017.04.081
16. Grishkov, V.N., Lotkov, A.I., Baturin, A.A., Cherniavsky, A.G., Timkin, V.N., and Zhapova, D.Y., Effect of recrystallization annealing on the inelastic properties of TiNi alloy under bending, *AIP Conf. Proc,* 2016, vol. 1783, article no. 020067. https://doi.org/10.1063/1.4966360

17. Poletika, T.M., Girsova, S.L., and Lotkov, A.I., Ti_3Ni_4 precipitation features in heat-treated grain/subgrain nanostructure in Ni-rich TiNi alloy, *Intermet,* 2020, vol. 127, article no. 106966. https://doi.org/10.1016/j.intermet.2020.106966

18. Ryklina, E.P., Prokoshkin, S.D., Chernavina, A.A., and Perevoshchikova, N.N., Investigation on the influence of thermomechanical conditions of induction and structure on the shape memory effects in Ti–Ni alloy, *Inorg. Mater.,*2010, vol. 1, no. 3, pp. 188–194. https://doi.org/10.1134/S2075113310030032

19. Otsuka, K. and Wayman, C., *Shape Memory Materials,* Cambridge: Cambridge Univ. Press, 1998.

20. Demers, V., Brailovski, V., Prokoshkin, S.D., and Inaekyan, K.E., Optimization of the cold rolling processing for continuous manufacturing of nanostructured Ti–Ni shape memory alloys, *J. Mater. Process. Technol.,* 2009, vol. 209, pp. 3096–3105. https://doi.org/10.1016/j.jmatprotec.2008.07.016

21. Valiev, R.Z., Gunderov, D.V., Lukyanov, A.V., and Pushin, V., G Mechanical behavior of nanocrystalline TiNi alloy produced by severe plastic deformation, *J. Mater. Sci.,* 2012, vol. 47, pp. 7848–7853. https://doi.org/10.1007/s10853-012-6579-8

22. Gunderov, D., Churakova, A., Lukyanov, A., Prokofiev, E., Pushin, V., Kreitcberg, A., and Prokoshkin, S., Features of the mechanical behavior of ultrafine-grained and nanostructured TiNi alloys, *Mater. Today: Proc.,* 2017, vol. 4, no. 3, pp. 4825–4829. https://doi.org/10.1016/j.matpr.2017.04.078

23. Kashin, O., Krukovskii, K., Lotkov, A., and Grishkov, V., Effect of true strains in isothermal ABC pressing on mechanical properties of Ti49.8Ni50.2 alloy, *Metals,* 2020, vol. 10, no. 10, no. 1313, pp. 1–13. https://doi.org/10.3390/met10101313

Translated by I. Moshkin